GRAPH-BASED GUIDE-WIRE SEGMENTATION THROUGH FUSION OF CONTRAST-ENHANCED AND FLUOROSCOPIC IMAGES

Nicolas Honnorat [1,2,3], *Régis Vaillant* [2], *Nikos Paragios* [1,3,4]

[1] Center for Visual Computing, Ecole Centrale de Paris, FR
[2] General Electric Healthcare, Buc, FR
[3] Equipe Galen, INRIA Saclay, Ile-de-France, FR
[4] Université Paris-Est, LIGM (UMR CNRS), Center for Visual Computing, Ecole des Ponts ParisTech, FR

ABSTRACT

In this paper, we present a novel method that fuses, through a graph matching, segmentation of the blood vessels in contrast-enhanced images with segmentation of the guide-wires in the fluoroscopic images. This is achieved through a bottom up approach that first extracts local geometric primitives of interest in both images. Fusion between two graphs built with these primitives is performed through spectral matching and allows the definition of an improved criterion of ordering of the wire primitives. Given such criterion, local ordering is used towards reconstruction of multiple curvilinear structures that inherit visual support from both images. An evaluation performed on a broad variety of clinical situations validates the effectiveness of our approach.

***Index Terms*—**

Curvilinear structures, discrete optimization, spectral methods, graph matching, guide-wire segmentation

1. INTRODUCTION

The segmentation of the guide-wires used during routine cardiac angioplasty interventions is an interesting clinical problem [1]. This task, in spite of strong connections to other well studied problems such as tree-structures segmentation and contour delineation is particularly difficult due to severe lack of visual support and due to the presence of confusing structures.

Let us briefly review methods proposed for detecting curvilinear structures (ridges) which have already been used for detecting guide-wires. Basic approaches exploit low-level measurements, like methods based on the Hessian eigenvalues: the main eigenvalue [1] or a "measure" combining them, like the vesselness [2]. The theory of steerable filters led also to a new class of filters exhibiting better results such as [3] exploited in [4].

This support can then be enhanced, for instance by Coherence-enhancing Diffusion [1] or Tensor Voting [5]. A promising alternative exploits machine learning methods for training detectors combining the output of simple filters like the previous one [4] or Haar Wavelets [6]. Such methods could produce more efficient detectors in the expense of generating a sizeable/representative database of positive examples.

The feature detection space serves then as basis to high-level reasoning for guide-wire delineation. Chaining methods agglomerate information starting from seed points towards complete recovery of the structure of interest. These methods, as well as their multiple hypothesis testing variants [7] have been mainly used for blood vessel segmentation. The second class of methods consists of bottom-up techniques, that extract primitives likely to belong to the wire and group them progressively. The grouping can be decided according to continuation criteria [4] or according to a function trained for this purpose [6]. It can be performed greedily [6] or by solving an optimization problems such as an ordering problem [4]. If the wire endpoints are known, shortest path/fast marching [8] techniques like [9] can also be exploited.

Despite promising results of these methods, fully- automated delineation of the guide-wire is often not feasible. Having said that, in such a clinical setting, cardiologists inject contrast agent to make blood vessels visible during the intervention. Such a valuable information has been ignored up to now, mostly due to the lack of correspondences between the fluoroscopic and the contrast enhanced images and the underlying non-rigid deformation.

In this paper, we present a novel bottom-up approach that begins with extracting line-segments from the fluoroscopic image where the guide-wire is visible and from blood vessel centerlines that are visible in a contrast-enhanced image. A graph is then built with each set of primitives and our method matches them in a way that creates robust, reliable shortcuts between neighboring segments in the fluoroscopic image through the contrast-enhanced image. These shortcuts are exploited by a novel variant of the linking algorithm [4] that we extended to the reconstruction of multiple guide-wires.

The remainder of this paper is organized as follows: in section 2 we describe our graph matching based approach for guide-wire segmentation. In section 3, we present the experimental validation that was carried out. Discussion concludes the paper.

2. GRAPH MATCHING FOR GUIDE-WIRE DELINEATION

2.1. Line segments extraction

Interest points are detected using steerable filters of different scales and orientations, both in the contrast enhanced and in the fluoroscopic images. The responses of the detector in the fluoroscopic images, where the signal to noise ratio is low, are enhanced by tensor-voting [5] as described in [10]. The outcome of this step consists in potential components of the guidewire in the fluoroscopic image, and consists in potential blood vessels centerlines in the contrast-enhanced image. These interest points are clustered in a fully unsupervised manner using geometric proximity (formation of local line-segments) as criterion [11] and represented compactly using a line being determined from a RANSAC variant [12].

This work was funded by ANRT grant 1062/2008, GE Healthcare, the European Research Council under the European Community's Seventh Framework Programme FP7/2007-2013/ERC grant 259112 and the ADOC grant of the Medicen Competitive Cluster of Ile-de-France region. We thank N. Komodakis for the clustering method.

In a given image space (we make no distinction between the two spaces and the same process is applied in both spaces independently), let us denote with p_i the pixels detected. Inspired by [4] we denote with θ_i the direction providing the best filter response. In addition, we consider the scale σ_i at which the point has been extracted. We generalize [4] to multi-scale segments extraction by first defining this novel proximity criterion for point clustering:

$$\delta\left(p_i, p_j\right) = \frac{d(p_i, p_j)}{\sigma_j} + \alpha e\left(p_i, \theta_i, p_j, \theta_j\right)$$

where $d(.,.)$ is the Euclidean distance and $e\left(p_i, \theta_i, p_j, \theta_j\right)$ denotes the scale invariant Elastica criterion [13] that has been made direction invariant by taking the minimum of the criterion over the four possible combinations of directions compatible with θ_i and θ_j.

The line-segments support is found by minimizing:

$$\begin{array}{ll} \texttt{min} & \sum_{x_{ij}\in\{0,1\}} x_{ij}\delta\left(p_i, p_j\right) \\ \text{s.t.} & \left\{ \begin{array}{ll} \sum_j x_{ij} = 1 & \forall i \\ x_{ij} \leq x_{jj} & \forall i, j \end{array} \right. \end{array}$$

where $\delta\left(p_j, p_j\right)$ penalizes the creation of a cluster of center p_j. We obtained multi-scale clusters by taking:

$$\delta\left(p_j, p_j\right) = {K^{LSE}}{\sigma_j}^2$$

Given our choice of proximity, this choice provides indeed clusters σ_j times larger and containing ${\sigma_j}^2$ times more elements when their center has been extracted at scale σ_j, like expected.

Outliers are collected into a cluster $\emptyset$, whose center lies at a proximity $\delta_\emptyset$ of each pixel. The optimization is performed by [11] and provides clusters at the same scale as their center pixel. We use this scale for fitting line-segments with [12], like in [4], using finally the same three parameters $(\alpha, K^{LSE}, \delta_\emptyset)$ for all images. [Fig. (1,3)] shows structure and centerline parts extracted by our algorithm.

2.2. Paths shortening graph fusion

Our graph fusion method matches the two lines segments sets previously extracted, with the aim of creating shortcuts between "neighbors" of the fluoroscopic image through the contrast-enhanced one. By the way, missing visual support of the wire can be partially recovered using the visual support of the enhanced blood vessels. Our method is based on spectral matching and penalizes the deformations between the two subsets of segments finally matched.

Let describe the graph construction that our method performs. Let us denote with $a_i = (a_i^1, a_i^2)$ the line-segments extracted in the fluoroscopic image and with b_j the blood vessels centerlines parts extracted in the contrast-enhanced image. Two graphs are built: G^A containing two nodes per segment a_i, corresponding to the two possible orientations: (a_i^1, a_i^2) and (a_i^2, a_i^1) ; and G^B, that is built in the same manner with b_j. For each segment i in G^A, $\bar{i}$ will denote the segment with opposite orientation. The "distance" matrix A of G^A is defined as follows (β_1, β_2 being parameters):

$$A_{kl} = \mu(\beta_1 d^s\left(k, l\right) + \beta_2 e^s\left(k, l\right)) \qquad \forall k, l \in G^A$$

where d^s is the Euclidean distance between the second extremity of k and the first extremity of l, where e^s is the (oriented) scale invariant Elastica [13] corresponding to this link and $\mu(.)$ discards edges with costs higher than a threshold K:

$$\mu(x) = \left\{ \begin{array}{ll} x & if\ x \leq K \\ \infty & otherwise \end{array} \right.$$

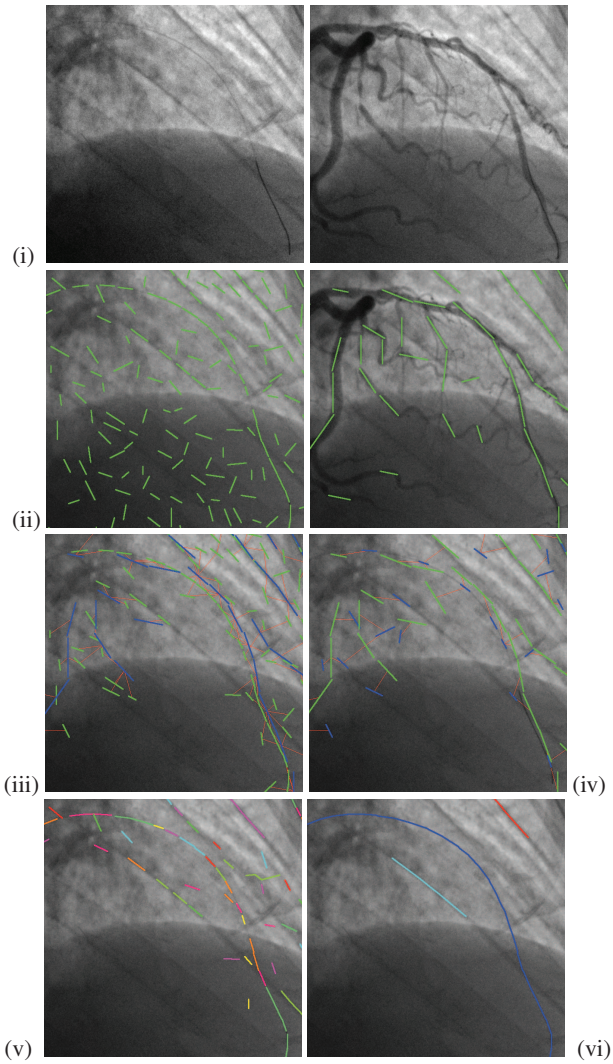


Fig. 1. (i) fluoroscopic and contrast-enhanced images (ii) line-segment extracted (iii) matching Φ: line-segment from the fluoroscopic image (in green) are matched with blood vessel centerlines parts (in blue) (iv) matching Ψ (between green centerlines and blue fluoroscopic line-segments) (v) output of the preliminary linking (vi) structures finally segmented

In order to favor segments with long support, we introduce a negative cost $\mathcal{C}(c_k)$ for each segment c_k that decreases with the length of c_k. The cost of a path in a graph is then given by the sum of the costs over the links and the nodes visited. We build a distance matrix B for G^B in the same manner and we use the Floyd Warshall algorithm for computing the matrix of shortest paths through G^B, C.

Our method aims at matching G^A and G^B with oriented arcs Φ from G^A to G^B and Ψ from G^B to G^A in a manner that shorten as much as possible all the best travels through G^B between neighbors in G^A. Without loss of generality, we cast this problem into:

$$\begin{array}{ll} \min\limits_{\phi_{i,j},\psi_{k,l}} & \sum\limits_{i,l\in G^A}\ \sum\limits_{j,k\in G^B} \phi_{i,j}\left[V_\phi(i,j) + C_{j,k} + V_\psi(k,l)\right]\psi_{k,l} \\ \text{s.t.} & \left\{ \begin{array}{ll} \sum_{j\in G^B} \phi_{i,j} = 1 & \forall i \\ \sum_{l\in G^A} \psi_{k,l} = 1 & \forall k \\ i\ and\ l\ are\ neighbors\ in\ G^A & \end{array} \right. \end{array}$$

where ϕ is a matching described by the boolean variables $\{\phi_{i,j}\}, \forall i \in G^A, \forall j \in G^B$, $V_\phi(i,j)$ denotes a travel cost from i in G^A to j in G^B, ψ describes a matching from G^B to G^A and is associated with the costs $V_\psi(k,l)$. Let us denote:

$$M_{i,j}^{k,l} = [V_\phi(i,j) + C_{j,k} + V_\psi(k,l)]$$

In order to address missing correspondences, let us introduce variables $\phi_{i,\emptyset}\ \forall i \in G^A$ and $\psi_{j,\emptyset}\ \forall j \in G^B$ and let denote:

$$\begin{array}{rcll} S & = & G^A \times G^B \ \cup\ G^A \times \{\emptyset\} \ \cup\ G^B \times G^A \ \cup\ G^B \times \{\emptyset\} & \\ S_i & = & \{i\} \times G^B \ \cup\ \{(i,\emptyset)\} & \forall i \in G^A \\ S^j & = & \{j\} \times G^A \ \cup\ \{(j,\emptyset)\} & \forall j \in G^B \end{array}$$

Spectral matching is attractive when the similarity matrix is sparse, what is the case for M. Therefore, we applied a gradient ascent method inspired by [14] to our problem. Our method relaxes the integrality constraint on the $\phi_{i,j}$ and $\psi_{k,l}$ and store all the variables in a vector of real numbers $x_m, m \in S$. We consider similarities of the following form (where K^{GF} discourages the matching):

$$N_{m,n} = \begin{cases} max(0, K - M_m^n) & if\ m \in G^A \times G^B, n \in G^B \times G^A \\ max(0, K - M_n^m) & if\ m \in G^B \times G^A, n \in G^A \times G^B \\ K^{GF} & if\ m = n, m \in G^A \times \{\emptyset\} \\ K^{GF} & if\ m = n, m \in G^B \times \{\emptyset\} \\ 0 & otherwise \end{cases}$$

Following the "tensor trick" [14], we introduce y_m such that $y_m = \sqrt{x_m}$, and we formulate our problem into the following form, that we solve using the gradient ascent method [14]:

$$\max_y \sum_{m,n \in S} [N_{m,n}]\, {y_m}^2 {y_n}^2$$

$$\text{s.t.} \quad \begin{cases} \sum_{m \in S_i} {y_m}^2 = 1 & \forall i \in G^A \\ \sum_{m \in S^j} {y_m}^2 = 1 & \forall j \in G^B \end{cases}$$

Although [14] do not provide guarantees on the maximum, experimental evidence demonstrated that the method converges to a reasonable optimum. Once the matchings Φ and Ψ have been determined (by considering the most important correspondence of each segment) the distance matrix of G^A is updated with the best travel costs through G^B, and symmetrized:

$$\begin{array}{rcl} D^*_{i,l} & = & min\left(A_{i,l}, \min\limits_{j,k \in G^B} [\Phi_{i,j} + C_{j,k} + \Psi_{k,l}]\right) \\ D_{i,l} & = & min\left(D^*_{i,l}, D^*_{l,i}\right) \end{array}$$

D is then used for delineating the wires. [Fig. (1)] presents matchings results and [Fig. (3)] shows "distance" reductions.

2.3. Multiple structure reconstruction

In order to cope with multiple structures, we adapted the ordering algorithm [4]. Our algorithm maintains a varying number of n_g sequences of inlier segments I_g, a list of outliers O and minimizes the energy:

$$E(I_g, O) = \sum_{g=1}^{n_g} \sum_{i=1}^{|I_g|-1} D_{I_g(i), I_g(i+1)} - \sum_{a \in O} \mathcal{C}(a) + n_g K^{MSR}$$

where $|I_g|$ denotes the length of I_g and $I_g(i)$ its element number i. The parameter K^{MSR} acts as a minimum description length criterion reducing the number of structures reconstructed.

	MDR	FDR	MDR^{all}	FDR^{all}
points	0.128	0.899	0.17	0.858
line-segments	0.246	0.862	0.299	0.818
line-segments chosen by the preliminary linking	0.274	0.667	0.334	0.578
final wire(s)	**0.275**	**0.243**	**0.323**	**0.36**
final wire(s) without preliminary linking	0.467	0.415	0.448	0.501

Table 1. Mean results of our approach. The preliminary linking reduced the cumulated computational time over all the 48 test sequences from 15100 to 19 seconds. MDR is the proportion of ground truth pixels lying at more than 5 pixels of the segmented wires and FDR the proportion of segmented structures lying at more than 5 pixels of the ground truth. All the finally segmented structures are used for measuring MDR^{all} and FDR^{all}, whereas only the first (constrained) wire is used for measuring MDR and FDR.

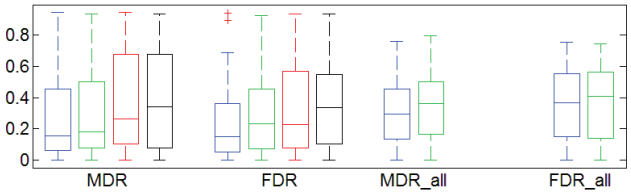


Fig. 2. the four different evaluations of our complete method (blue), without image fusion (green), with image fusion but single wire delineation [4] (red), without image fusion and with [4] (black).

We address this ordering problem by moving and exchanging subsequences from the I_g and from O like [4]. We introduce only two novel operations: one that creates a new sequence with a subsequence of O when it leads to a cost reduction higher than K^{MSR} (and supposed to be guide-wires) and the other removing inlier sequences that have lost their interest. We adapted all these operations for being able to impose the endpoints of the first guide-wire.

Assuming that G^A does not contain a negative circuit, we also propose a preliminary linking stage, that both reduces the computational burden and increases the robustness of the structure reconstruction with respect to outliers. The procedure computes first a potential $\mathcal{U}$ initialized with the costs $\mathcal{C}(i)$ for each i in G^A and applies the following operation until convergence:

$$\mathcal{U}(i) \leftarrow min\left(\mathcal{U}(i), \min_{j \in G^A} \mathcal{C}(i) + D_{j,i} + \mathcal{U}(j)\right)$$

$\mathcal{U}(i)$ is then the cost of the most interesting structure in G^A ending with i. Besides, the endpoint of a structure is necessarily a segment i such that $\mathcal{U}(\bar{i}) \geq 0$ (linking paths leading to $\mathcal{U}(\bar{i})$ and $\mathcal{U}(i)$ would otherwise creates a structure with lower cost). Taking these two conditions into account, we restricted ourselves to a small number of candidate structure endpoints, necessarily containing the extremities of the wires. We considered as outliers the segments that were not part of the corresponding paths and by considering the sequences of line-segments appearing in the same manner in different paths only once, we reduced the computational burden. [Fig. (1)] shows the output of this procedure and [Tab. (1)] presents quantitative results in favor of this approximation.

3. EXPERIMENTAL VALIDATION

Experimental validation was performed on 80 clinical interventions. 32 were used for parameter settings and the 48 remaining for evalua-

tion. For each intervention, one fluoroscopic image and one contrast-enhanced image corresponding to the same moment in the cardiac cycle were considered. The endpoints of the most interesting wire were provided to the algorithm. Results were measured in terms of missed detection rate (MDR) and false detections rate (FDR) at 5 pixels (1mm) [4, 6]. In order to take the presence of multiple structures into account, we have also annotated other structures of interest (other wires, catheters) and compared all the structures segmented with this ground truth, obtaining $\mathrm{MDR}^{\mathrm{all}}$, $\mathrm{FDR}^{\mathrm{all}}$. We chose transition costs V_ϕ and V_ψ of the same form:

$$V_\phi(i,j) = V_\psi(j,i) = \gamma_1 d^m(i,j) + \gamma_2(1 - cos(i,j))$$

where d^m denotes the Euclidean distance between the centers of the segments i and j, $cos(i,j)$ the cosinus of the angle between them and $(\gamma_1, \gamma_2) = (0.5, 100)$. We used the following segment cost, where $\mathcal{L}(c_k)$ denotes the length of c_k: $\mathcal{C}(c_k) = -0.5\,\mathcal{L}(c_k)$

We extracted 1400 points for an image of size 512×512 (adapting this number to the area of the image) from a grid of step 3 for fluoroscopic images and of step 5 for enhanced images. The guide-wires were extracted at scale $\sigma_F = 2$ and the blood vessels at scales $\sigma_E = \{3, 5\}$. For line-segment extraction, we chose $(\alpha, K^{LSE}, \delta_\emptyset) = (10, 275, 150)$. $(\beta_1, \beta_2, K^{GF}) = (0.01, 30, 185)$ defined the travel costs through the graphs G^A and G^B. $K = 200$ was used to determine the neighbors of a segment in these graphs, and K^{MSR} was set to 25.

[Tab. (1)] presents a comparison with a variant of [4] taking the endpoints constraint into account. Our set of parameters lead to the extraction of most of the wire support, but also of many outliers. In this context, the preliminary linking (that dramatically reduces the computational time) as well as the delineation of multiple structure clearly improves the results. The graph fusion introduced a modest quantitative improvement, in spite of qualitatively promising shortcuts selection [Tab. (1)].

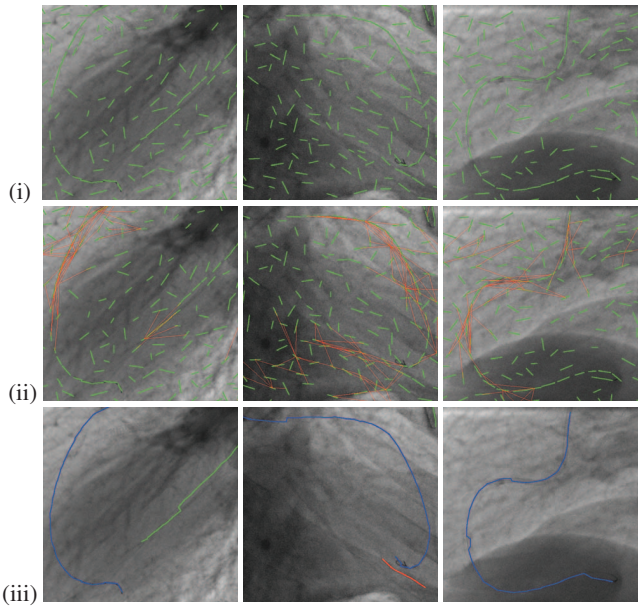


Fig. 3. (i) line-segment extracted in the fluoroscopic image (ii) costs reduced by the graph fusion (in red) (iii) structures finally segmented

4. DISCUSSION

In this paper, we have presented a novel algorithm exploiting contrast-enhanced images for improving the segmentation of guide-wires in fluoroscopic images through graph matching. Our method extracts line-segments from both images, build one graph of neighboring segments for each image and matches them by solving an optimization problem aiming at creating shortcuts through the more reliable graph/image. A reconstruction algorithm exploiting these linking costs is then applied, that simultaneously finds the optimal number of structures to reconstruct, the line-segments part of them and their optimal ordering. We have also reduced the computational burden of our segmentation method by introducing a preliminary linking stage that removes outliers as well. Our method is flexible and could incorporate higher order matching costs as well. In the future, we will apply our approach to other situations where multimodal combination of contour information is valuable.

5. REFERENCES

[1] S. A. M. Baert, M. A. Viergever, and W. J. Niessen, "Guide-wire tracking during endovascular interventions," *IEEE TMI*, vol. 22, no. 8, pp. 965–972, aug. 2003.

[2] A. F. Frangi, W. J. Niessen, K. L. Vincken, and M. A. Viergever, "Multiscale vessel enhancement filtering," in *MICCAI*, 1998.

[3] M. Jacob and M. Unser, "Design of steerable filters for feature detection using Canny-like criteria," *IEEE PAMI*, vol. 26, no. 8, pp. 1007–1019, 2004.

[4] N. Honnorat, R. Vaillant, and N. Paragios, "Guide-wire extraction through perceptual organization of local segments in fluoroscopic images," in *MICCAI*, 2010.

[5] E. Franken, P. Rongen, M. van Almsick, and B. M. ter Haar Romeny, "Detection of electrophysiology catheters in noisy fluoroscopy images," in *MICCAI*, 2006, pp. 25–32.

[6] A. Barbu, V. Athitsos, B. Georgescu, S. Boehm, P. Durlak, and D. Comaniciu, "Hierarchical learning of curves application to guidewire localization in fluoroscopy," in *CVPR*, 2007.

[7] O. Friman, M. Hindennach, C. Khnel, and H.-O. Peitgen, "Multiple hypothesis template tracking of small 3D vessel structures," *Med. Image Analysis*, vol. 14, pp. 160–171, 2010.

[8] T. Deschamps and L. D. Cohen, "Fast extraction of minimal paths in 3D images and applications to virtual endoscopy," *Medical Image Analysis*, vol. 5, pp. 281299, 2001.

[9] P. Wang, W.-S. Liao, T. Chen, S. K. Zhou, and D. Comaniciu, "Graph based interactive detection of curve structures in 2D fluoroscopy," in *MICCAI*, 2010.

[10] N. Honnorat, R. Vaillant, and N. Paragios, "Graph-based geometric-iconic guide-wire tracking," in *MICCAI*, 2011.

[11] N. Komodakis, N. Paragios, and G. Tziritas, "Clustering via LP-based stabilities," *NIPS*, 2008.

[12] P. Torr and A. Zisserman, "Robust computation and parametrization of multiple view relations," in *ICCV*, 1998.

[13] E. Sharon, A. Brandt, and R. Basri, "Completion energies and scale," *IEEE PAMI*, vol. 22, no. 10, pp. 1117–1131, 2000.

[14] O. Duchenne, F. Bach, I. Kweon, and J. Ponce, "A tensor-based algorithm for high-order graph matching," in *CVPR*, 2009.